Supporting Information

Synchrotron X-ray-Induced Photoreduction of Ferric Myoglobin Nitrite Crystals Gives the Ferrous Derivative with Retention of the O-bonded Nitrite Ligand†

Jun Yi,[‡] Allen M. Orville,[§] John M. Skinner,[§] Michael J. Skinner,[¶] George B. Richter-Addo[‡]*

[‡] *Department of Chemistry and Biochemistry, University of Oklahoma, 620 Parrington Oval, Norman OK 73019,*

[§] *Biology Department, Brookhaven National Laboratory, Upton, NY 11973-5000, and*

[¶] *High School Research Program, Brookhaven National Laboratory, Upton, NY 11973-5000.*

Materials and Methods

The hh aquometMb crystals were grown by the hanging drop vapor diffusion method at room temperature (~22 ^{o}C) as previously described (*1*). The ferric Mb-nitrite derivative was obtained by soaking the crystals in cryoprotectant [3.0 M ammonium sulfate; 100 mM Tris-buffer at pH 7.4; 10% glycerol] containing 0.35-0.5 M sodium nitrite for 10 min as previously described (*2*). The crystals were harvested with cryo-loops and flash-frozen in liquid nitrogen prior to data collection.

Single-crystal spectroscopy correlated with X-ray diffraction at beamline X26-C at the NSLS at BNL

Some of the instrumentation and methodology for the single-crystal optical absorption microspectrophotometry has been described (*3*). The software to control the Ocean Optics USB 4000 in EPICS was provided by David Beauregard at the Canadian Light Source and modified to interface with the X26-C beamline control software (CBASS) at Brookhaven National Laboratory by three of the authors (AMO, JMS, and MJS). Typical single-crystal spectroscopy data were collected by focusing the visible light to a ~25 μm diameter spot size that was aligned to the crystal eucentric rotation point and perpendicular to the X-ray beam path. The Ocean Optics USB 4000 spectrometer integration time (~100 – 250 ms) and box car (5-10 pixels) settings were adjusted to yield maximum sensitivity and signal to noise. The typical experiment involves the following steps:

1. A crystal is mounted and centered to the X-ray beam and within the cold stream with the Crystal Logic (Los Angeles, CA) diffractometer.
2. 72 digital images of the loop/crystal, one every 5° around a full 360° rotation are recorded. At each of the 72 orientations, an optical absorption spectrum is also measured.
3. CBASS calls the C3D algorithm (*4*) which determines the broadest, flat face of the loop/crystal and directs the goniometer to rotate the crystal so that this face is presented to the incident objective lens for spectroscopy. This establishes the "best" spectroscopy angle for the cryoloop and the crystal. It also has the greatest potential to avoid the cryoloop, which introduces spectral artifacts as it passes through the spectroscopy visible light path. The "best" angle determined by C3D is passed to CBASS for use during correlated data collection of absorption spectra and X-ray diffraction.
4. The optical spectra and the crystal images are combined into a side-by-side animated GIF and linked to the beamline database tracking software (PXdb). Because macromolecular

crystals often yield anisotropic optical spectra, an interactive JAVA movie application is also prepared that provides a means to examine the spectra and the crystal image as a function of rotation angle. In the animated GIF and the interactive JAVA movie, the crystal image correlates to the absorption spectrum such that the image is shown from the perspective of the spectroscopy photons passing through the crystal. Based upon inspection of the JAVA movie, the user may select an alternative angle for correlated spectroscopic and X-ray data collection.

5. During correlated spectroscopic and X-ray diffraction data collection, the crystal is first rotated to either the "best" or selected angle, a spectrum is recorded, and plotted in a terminal window. The crystal then rotates to the desired goniometer angle to start the X-ray diffraction data collection. During the readout loop of the X-ray detector and while the X-ray shutter is closed, the crystal is rotated back to the "best" or selected orientation, another optical spectrum is recorded, and the result is plotted as an overlay of the first spectrum. CBASS then continues executing the X-ray diffraction data collection strategy at the appropriate rotation angle. This method automatically measures optical spectra after every image for the first 15 images, and then after every tenth image thereafter. Thus, a family of optical spectra is obtained as a function of X-ray exposure wherein each spectrum differs from the others by the cumulative X-ray exposure established by the diffraction data collection strategy. At the end of the X-ray diffraction data collection, the resulting optical data is linked to the PXdb in several file formats.
6. The optical data are collated and processed for submission to the PDB with the coordinates of the structure determined from the particular crystal. Therefore, PDB code 3LR9 is linked to the family of absorption spectra obtained during the X-ray diffraction data collection.

X-ray diffraction data collection and processing

Home source diffraction data: X-ray diffraction data at the University of Oklahoma were collected at 100 K on a RigakuMSC RU-H3R X-ray generator operated at 48 kV/98 mA to produce Cu/Kα radiation (λ = 1.5418 Å). 1° oscillation images were collected over a range of 160° with an exposure time of 6 min per image and a crystal-to-detector distance of 75 mm. Diffraction data were indexed and processed with the d*TREK program (Macintosh v.99D) (*5*).

Synchrotron diffraction data: X-ray diffraction data were collected at the National Synchrotron Light Source (NSLS) at the Brookhaven National Laboratory. The data were collected at 100 K on beamline X26-C using an ADSC Quantum 4 CCD detector. 1° oscillation images were collected over a range of 365° with an exposure time of 10 seconds per image and a crystal-to-detector distance of 130 mm. Diffraction data from images 161 to 365 were indexed and processed with the d*TREK program (Macintosh v.99D) (*5*). The program RADDOSE (*6*) was used to estimate the total X-ray dose during the data collection period.

Structure solution and refinement

Home source data: The phase information was obtained using the molecular replacement method as implemented in *PHASER* (v1.3.3) (*7*). The search model was the 1.45 Å resolution structure of hh MbCO (PDB access code 1DWR) with all solvent molecules, carbon monoxide and sulfate ions removed. Restrained refinement was carried out for 25 cycles prior to the addition of any solvent, ligand, or sulfate ion, and this resulted in a drop of *R*-factor to 24.1% from an initial value of 28.3%. The program SMILES (in *COOT* (*8*)) was used to generate the

anionic nitrite fragment labeled as filename NO2. This NO2 fragment was placed into the positive electron density observed in the distal pocket in the F_o-F_c map. The bond distance and bond angle for the nitrite anion used in the refinement were taken from the published crystal structure of sodium nitrite (O-N = 1.24 Å; ∠ONO = 115°) (*9*). The ligand cif file was used in the subsequent real space refinement to model the NO2 into the positive electron density, and the resulting coordinates merged with the protein coordinates. Two other nitrite anions were similarly modeled in the crystal lattice based on the F_o-F_c map. The sulfate anion ligand file was imported from the *COOT* database; two sulfate anions were added to the model based on the F_o-F_c electron density map.

An additional 45 cycles of restrained isotropic refinement were run to give an *R*-factor of 23.0%. The Fe–(nitrite) bond distance and angle parameters were unrestrained throughout the refinement; however, internal restraints of 1.24(2) Å (for d(N-O)) and 115(5)° (for ∠ONO) were applied to the nitrite groups. The structure was checked for sidechains showing low occupancy or multiple conformations. Lysine 50 was modeled at 50%, and Lysine 77 was modeled in two conformations with equal occupancies (50% each). The two sulfate anions were modeled in 80% and 60% occupancies. The C-terminal residues Gln152 and Gly 153 were omitted from the structural model due to their poor observed electron density. Water molecules were added using Find Waters in *COOT* PHENIX refinement (*10*) and model manipulation using *COOT* were carried out. The crystallographic *R* and R_{free} for the final model are 19.3% and 24.8%, respectively, in the 21.85-1.60 Å range. The ferric hh Mb(ONO) protein crystallizes with one molecule in the asymmetric unit, and the final model of its structure contains 151 amino acid residues, one heme group, three nitrite anions, two sulfate anions, and 97 water molecules.

Synchrotron data: The phase information was obtained using the molecular replacement method as implemented in *PHASER* (v1.3.3) (*7*). The search model was the 1.45 Å resolution structure of hh MbCO (PDB access code 1DWR) with all solvent molecules, carbon monoxide and sulfate ions removed. Restrained isotropic refinement was carried out for 25 cycles prior to the addition of any solvent, ligand, or sulfate ion, and this resulted in a drop of the R-factor to 23.8% from an initial value of 28.1%. The NO2 ligand.cif file (described previously) was used for the modeling of nitrite in the structure. The Fe–(nitrite) bond distance and angle parameters were unrestrained throughout the refinement; however, internal restraints of 1.24(2) Å (for d(N-O)) and 115(5)° (for ∠ONO) were applied to the nitrite groups. Four nitrite anions (one bound to Fe center and other three in the crystal lattice) and two sulfate anions were added to the model based on density seen in an F_o-F_c electron density map. An additional 50 cycles of restrained refinement were run to give an R-factor of 22.9%. The structure was checked for sidechains showing low occupancy or multiple conformations. Lysine 50 was modeled at 50%, and Lysine 77 was modeled in two conformations with occupancies of 32% and 68%. Two sulfate anions were modeled in with occupancies of 80% and 60%. Poor electron density was observed at the C-terminus of the protein for residues Gln152 and Gly 153, and Gly 153 was omitted from the structural model. Water molecules were added using Find Waters in *COOT* (*8*). PHENIX refinement (*10*) and model manipulation using COOT were carried out, which gave the crystallographic *R* and R_{free} (for the final model) 17.9% and 21.2%, respectively, in the 26.7-1.55 Å range. The protein crystallizes with one molecule in the asymmetric unit, and the final model of its structure contains 152 amino acid residues, one heme group, four nitrite anions, two sulfate anions, and 123 water molecules.

The $2F_o$-F_c and F_o-F_c electron density maps were generated using *FFT* as implemented in *CCP4* (*11*). The $2F_o$-F_c and F_o-F_c electron density maps and the final models of the heme sites of the hh Mb nitrite structures are shown in Figures 3 and 4, which were drawn using PyMOL (Delano Scientific, 2006: http://www.pymol.org) and labels were added using Adobe® Photoshop.

Table S1. X-ray data collection and refinement statistics[a]

	Mb^{III}(ONO)	Mb^{II}(ONO)*
PDB access code	3LR7	3LR9
A. Crystal parameters		
Space Group	$P2_1$	$P2_1$
Unit cell dimensions *a*, *b*, *c* (Å),	35.27, 28.53, 62.93,	35.33, 28.69, 62.91,
β (°)	105.4	105.6
Molecules per asym. unit	1 monomer	1 monomer
Solvent content (%)	33.68	34.07
B. Data collection		
Wavelength (Å)	1.5418	1.00
Temperature (K)	100	100
Resolution range (Å)	21.85-1.60	26.74-1.55
Number of observations	47739	68896
Unique reflections	15927	17892
Multiplicity	3.0(2.96)	3.85(2.87)
Completeness (%)	98.0(96.0)	99.2(95.3)
Mean $I/\sigma(I)$	9.9(3.0)	15.7(3.9)
R_{merge} (%)[b]	5.6(29.8)	4.2(18.6)
C. Refinement		
Resolution (Å)	1.60	1.55
Number of protein atoms	1234	1243
Number of heteroatoms	116	146
R-factor (%)[c]	19.3	17.9
R_{free} (%)[d]	24.8	21.2
Average B-factors (Å^2)	22.21	15.6
r.m.s.d.s from standard geometry		
Bond lengths (Å)	0.007	0.006
Bond angles (°)	0.97	0.98
Ramachandran plot (%)		
Most favored region	97.3	98.0
Allowed region	2.7	2.0
Disallowed region	0	0

[a] The data in brackets refer to the highest resolution shell.
[b] $R_{merge} = \sum| I - \langle I \rangle ||/\sum(I)$ Where I is the individual intensity observation and $\langle I \rangle$ is the mean of all measurements of I.
[c] $R = \sum||F_o|- |F_c||/\sum|F_o|$ where F_o and F_c are the observed and calculated structure factors, respectively.
[d] R_{free} was calculated using 5% of the randomly selected diffraction data which were excluded from the refinement.

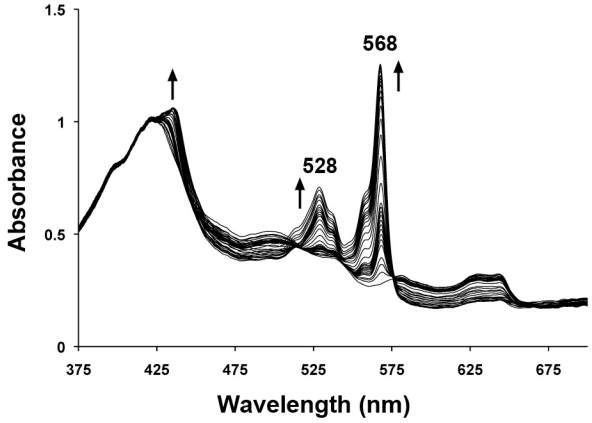

Figure S1. Single-crystal UV-vis spectra (~25 μm incident light focal spot size) of aquometMb at 100 K exposed to high-intensity X-rays over a 95 min period. The first 15 spectra were collected after each image frame (15 s exposure per frame) and the remaining spectra collected after each set of 10 frames. The red shift of the Soret band, and the appearance and shape of the peaks at 528 nm (with a shoulder at 536 nm) and at 568 (with a shoulder at 556 nm) are similar to those published for the photoreduction of $Mb^{III}(H_2O)$ to the ferrous $Mb^{II}(H_2O)$ derivative (at 528/536 nm and 556/566 nm, respectively) (*12-14*).

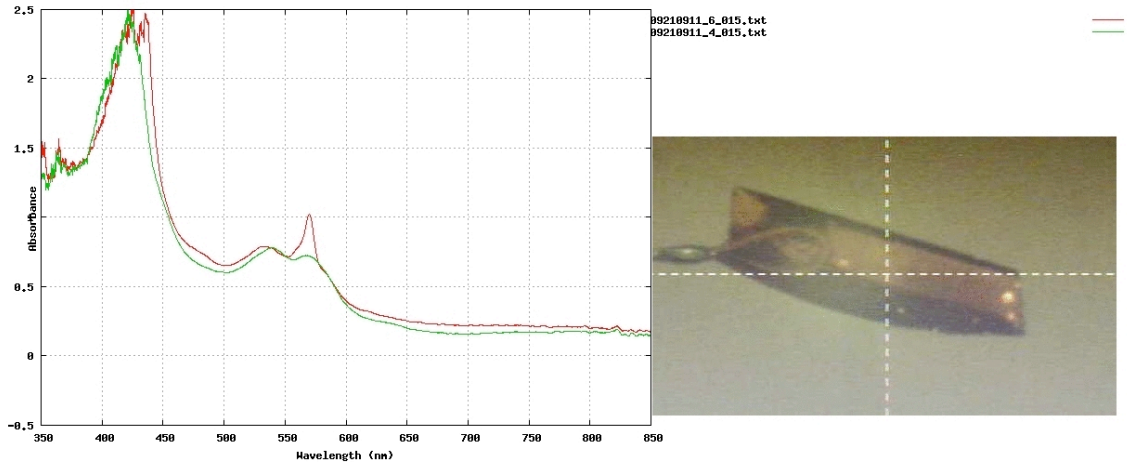

Figure S2. The single-crystal absorption spectra of ferric $Mb^{III}(ONO)$ before exposure to X-rays (green trace) and after exposure to high-intensity X-rays (red trace). An animated movie of the spectra as a function of crystal rotation angle is available under filename (Figure_4_animation.avi) submitted separately.

REFERENCES

1. Chu, K., Vojtchovsky, J., McMahon, B. H., Sweet, R. M., Berendzen, J., and Schlichting, I. (2000) Structure of a Ligand-Binding Intermediate in Wild-Type Carbonmonoxy Myoglobin, *Nature 403*, 921-923.
2. Copeland, D. M., Soares, A., West, A. H., and Richter-Addo, G. B. (2006) Crystal Structures of the Nitrite and Nitric Oxide Complexes of Horse Heart Myoglobin, *J. Inorg. Biochem. 100*, 1413-1425.
3. Orville, A. M., Lountos, G. T., Finnegan, S., Gadda, G., and Prabhakar, R. (2009) Crystallographic, Spectroscopic, and Computational Analysis of a Flavin C4a-Oxygen Adduct in Choline Oxidase, *Biochemistry 48*, 720-728.
4. Lavault, B., Ravelli, R. B., and Cipriani, F. (2006) C3D: A Program for the Automated Centering of Cryocooled Crystals, *Acta Cryst. D62*, 1348-1357.
5. Pflugrath, J. (1999) The Finer Things in X-Ray Diffraction Data Collection, *Acta Cryst. D55*, 1718-1725.
6. Paithankar, K. S., Owen, R. L., and Garman, E. F. (2009) Absorbed Dose Calculations for Macromolecular Crystals: Improvements to RADDOSE, *J. Synchrotron Rad. 16*, 152-162.
7. McCoy, A. J., Grosse-Kunstleve, R. W., Adams, P. D., Winn, M. D., Storoni, L. C., and Read, R. J. (2007) *PHASER* Crystallographic Software, *J. Appl. Cryst. 40*, 658-674.
8. Emsley, P., and Cowtan, K. (2004) COOT: Model-Building Tools for Molecular Graphics, *Acta Cryst. D D60*, 2126-2132.
9. Carpenter, G. B. (1955) Further Least-Squares Refinement of the Crystal Structure of Sodium Nitrite, *Acta Cryst. 8*, 852-853.
10. Adams, P. D., Grosse-Kunstleve, R. W., Hung, L.-W., Loerger, T. R., McCoy, A. J., Moriarty, N. W., Reed, R. J., Sacchettini, J. C., Sauter, N. K., and Terwilliger, T. C. (2002) PHENIX: Building New Software for Automated Crystallographic Structure Determination, *Acta Cryst. D58*, 1948-1954.
11. Bailey, S. (1994) The CCP4 Suite: Programs for Protein Crystallography, *Acta Cryst. D50*, 760-763.
12. Lamb, D. C., Ostermann, A., Prusakov, V. E., and Parak, F. G. (1998) From Metmyoglobin to Deoxy Myoglobin: Relaxations of an Intermediate State, *Eur. Biophys. J. 27*, 113-125.
13. Engler, N., Ostermann, A., Gassmann, A., Lamb, D. C., Prusakov, V. E., Schott, J., Schweitzer-Stenner, R., and Parak, F. G. (2000) Protein Dynamics in an Intermediate State of Myoglobin: Optical Absorption, Resonance Raman Spectroscopy, and X-Ray Structure Analysis, *Biophys. J. 78*, 2081-2092.
14. Beitlich, T., Kuhnel, K., Schultze-Briese, C., Shoeman, R. L., and Schlichting, I. (2007) Cryoradiolytic Reduction of Crystalline Heme Proteins: Analysis by UV-Vis Spectroscopy and X-ray Crystallography, *J. Synchrotron Rad. 14*, 11-23.